

## Investigating the role of soil fabric in unsaturated soils

Mohammad Motaleb Nejad, S.M. ASCE<sup>1</sup> and Kalehiwot Nega Manahiloh, M. ASCE<sup>2</sup>

<sup>1</sup> Research Assistant, Dept. of Civil and Environmental Engineering, University of Delaware, 301 DuPont Hall, Newark, DE 19716, U.S.A.; email: [mohmtlb@udel.edu](mailto:mohmtlb@udel.edu)

<sup>2</sup> Assistant Professor, Dept. of Civil and Environmental Engineering, University of Delaware, 301 DuPont Hall, Newark, DE 19716, U.S.A.; email: [knega@udel.edu](mailto:knega@udel.edu)

### ABSTRACT

The principle of effective stress states that the strength and volume change behaviors of soil are governed by intergranular forces expressed in terms of a continuum quantity called effective stress. Past research on effective stress formulations has identified a tensorial quantity that characterizes the liquid phase of unsaturated granular geomaterials. This quantity was named fabric tensor of the liquid phase and was shown to be anisotropic and to have an intrinsic association with the evolution of the effective stress tensor. It was also shown that its variation is random and can be depicted with microstructural image analysis. In this study, two past micromechanical effective stress formulations are discussed in comparison with Bishop's effective stress. The extended Mohr-Coulomb and effective stress approaches are used in interpreting shear strength parameters and effective stress parameter for partially saturated granular soils. Correlations are identified for some material variables. The nonlinearity observed in the angle of friction associated with the matric suction was discussed in relation to the fabric tensor of the liquid phase.

### Citation information: please cite this work as follows

Motaleb Nejad, M. and Manahiloh K.N., *Investigating the Role of Soil Fabric in Unsaturated Soils*, in Geotechnical Frontiers 2017: Geotechnical Materials, Modeling, and Testing, GSP 280.

**Link to published article:** <https://ascelibrary.org/doi/10.1061/9780784480472.063>

## INTRODUCTION

Nearly a century has passed from the first time that Terzaghi (1925) (Terzaghi 1925) proposed his "effective stress" in soil mechanics. He defined effective stress as the stress that governs the volumetric and strength behavior of a two-phase-soil, consists of a liquid phase and a rigid solid phase. He described the effective stress as the difference between total stress and pore water pressure. Although, his effective stress is instrumental in capturing the behavior of two-phase-soils, the definition of effective stress for unsaturated soils has remained challenging.

The shear strength of a saturated soil can be described using the Mohr-Coulomb criterion and the effective stress variable as (Terzaghi 1939):

$$\tau_f = c' + (\sigma')_f \tan \phi' = c' + (\sigma - u_w)_f \tan \phi' \quad (1)$$

In Equation (1):  $\tau_f$ ,  $c'$ ,  $(\sigma - u_w)_f$ , and  $\sigma$  and are the shear stress, effective cohesion, effective normal stress, and total normal stress at failure, respectively.  $\phi'$  is the effective angle of internal friction.

For unsaturated soils, the failure criterion should capture the transition from saturated zone to partially saturated zone, and different degrees of saturation as well. Blight (1967) performed a series of consolidated-drained triaxial tests for unsaturated silt showed that, as the water inside the soil dries out and matric suction is introduced to the soil, the stress associated with failure increases to higher values. This observation, shown schematically in Figure 1, suggests that soils have higher strength when unsaturated.

In an attempt to forward a quantity similar to Terzaghi's effective stress, Bishop (1959) proposed effective stress equation that accounts for the negative water pressure that presents in partially saturated soil:

$$\sigma'_f = (\sigma - u_a)_f + \chi_f (u_a - u_w)_f \quad (2)$$

In Equation 3,  $\chi$  is a material parameter that varies among different soils. Jennings and Burland (1962) performed a series of oedometer tests and reported that the volumetric behavior of the soil cannot be captured with Bishop's effective stress. They showed that the soil undergoes a significant reduction in volume when it is soaked suddenly (i.e. collapsing behavior).

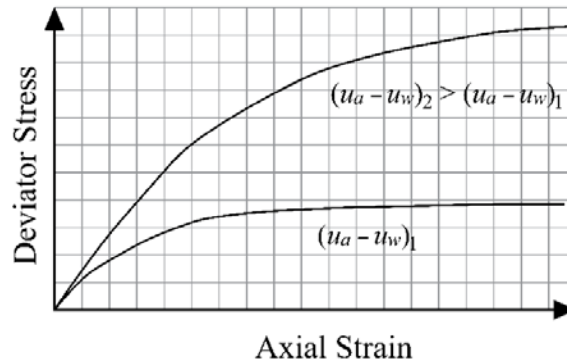


**Figure 1. Change in strength behavior of soil with different matrix suctions ( $u_a - u_w$ ).**

Bishop and Blight (1963) proposed an indirect method to obtain  $\chi$  for soils. In their method,  $\chi$  was estimated at failure conditions. It means that it is not possible to obtain  $\chi$  unless unsaturated soil tests are performed up to failure and some sort of a failure criterion is adopted.

Fredlund and Morgenstern (1977) criticized the equation proposed by Bishop, from independent state variable point of view. They emphasized that the inclusion of a material variable (i.e.  $\chi$ ) makes Bishop's effective stress a material-dependent state variable. They introduced three independent stress state variables,  $(u_a - u_w)$ ,  $(\sigma - u_a)$  and  $(\sigma - u_w)$ , and highlighted that two of the three can be combined to capture the strength and volumetric behavior of an unsaturated soil.

Fredlund et al. (1978) Extended Mohr-Coulomb criterion (Equation 3) for unsaturated soil based on the observed influence of matric suction on shear strength of soils. They proposed that, as soil dries out, the increase in matric suction introduces an apparent cohesion on top of the intrinsic cohesion of the soil.

$$\tau_f = c' + (u_a - u_w)_f \tan \phi^b + (\sigma - u_a)_f \tan \phi' \quad (3)$$

In the equation  $c'' = c' + (u_a - u_w)_f \tan \phi^b$  is called apparent cohesion. Figure 2 illustrates the simplified boundaries for the Extended Mohr-Coulomb failure surface. Note in Figure 2 that, when soil is saturated,  $(u_a - u_w) = 0$  and therefore, Equation 3 reduces to the conventional Mohr-Coulomb failure criterion of saturated soil.

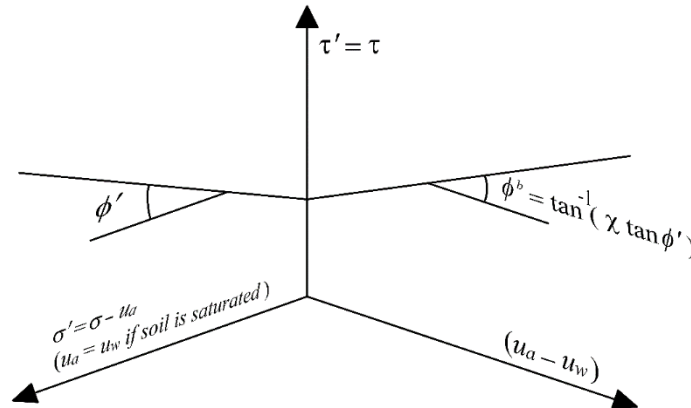


**Figure 2. Boundaries of the Extended Mohr-Coulomb failure envelop.**

Vanapalli et al. (1996) showed that the angle of friction in the matric suction plane,  $\phi^b$ , in the extended Mohr-coulomb envelop becomes nonlinear once the matric suction surpasses the air-entry suction of a soil. This non-linear behavior is illustrated in Figure 3.

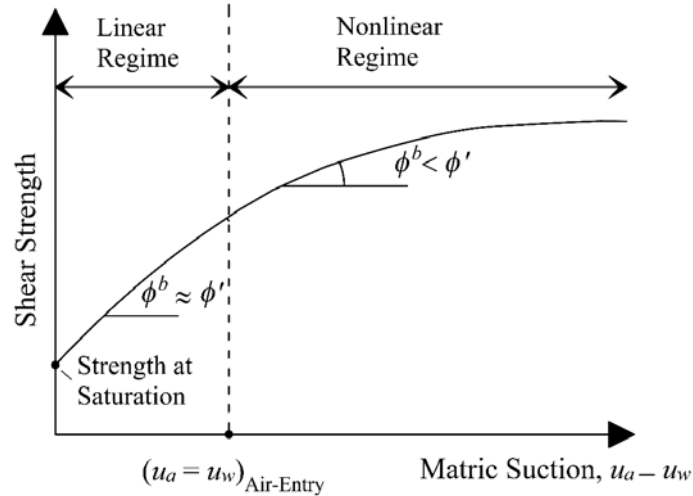


**Figure 3. Nonlinearity of  $\phi$ . (modified from Vanapalli et al. (1996)).**

In this study, we aim at comparing and relating, the extended Mohr-Coulomb criterion with a similar criterion obtained by using the effective stress approach. For the effective stress, we have adopted a microstructural-based effective stress formulation that was forwarded by previous researchers (Li 2003a). We have attempted to develop correlations between the angles of friction in the net stress and matric suction planes with the fabric tensor of the liquid phase.

### MICROMECHANICAL EFFECTIVE STRESS EQUATIONS

Li (2003a) performed a micromechanical analysis to derive a quasi-effective stress equation for unsaturated soil. He used a multi scaling method to describe the microstructure of the unsaturated soil. Figure 4 shows stress state for unsaturated soil at different scales. The concept of representative volume element (RVE) provides a tool for mathematical analysis in continuum mechanics. RVE is the smallest scale of a continuum that is representative of the whole continuum. For an idealized unsaturated granular soil, Figures 4a and 4b show stresses acting on an RVE and on the surface of a particle, respectively. Figure 4c shows the geometric boundaries for different phases of an unsaturated soil.

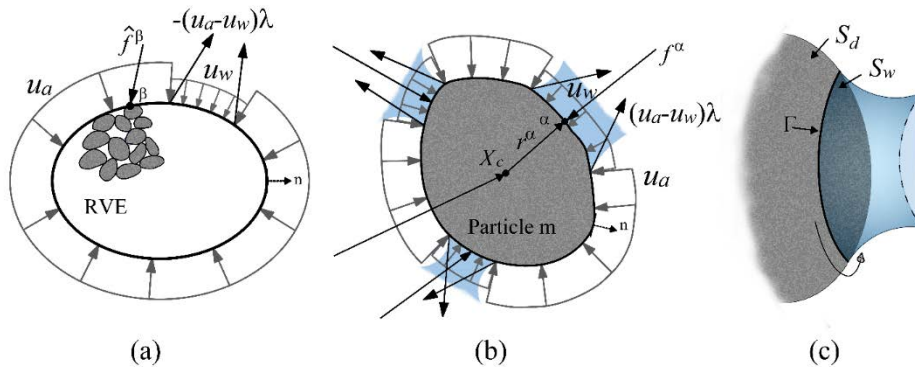


**Figure 4. stress state for unsaturated soil at different scales (a) RVE scale (b) Particle level (c) geometric boundaries for different phases of unsaturated soil.**

Assuming a smooth linear function (i.e. a first order approximation) for displacements of a point (such as point  $\alpha$ ) in Figure 4(b), and assuming that the resultant moment for a particle in equilibrium to be equal to zero, Li (2003a) wrote the total virtual work done in the RVE as sum of virtual works done by three sources; *internal contact forces* ( $f^\alpha$ ), *boundary contact forces* ( $\hat{f}^\beta$ ), and *pore pressure* ( $p_i$ ) on particle surfaces. Total virtual work equation was given as:

$$\sum_{m=1}^{N^p} \sum_{\alpha=1}^{N^m} f_j^{m\alpha} r_i^{m\alpha} = \sum_{\beta=1}^k \hat{f}_j^\beta x_i^\beta + \sum_{m=1}^{N^p} x_i^{c_m} \int_{S^m} p_j dA \quad (4)$$

Where  $N^p$  and  $N^m$  are the number of particles in the RVE, and the number of contacts on particle  $m$ , respectively.  $f_j^{m\alpha}$  and  $r_i^{m\alpha}$  denote the force on point  $\alpha$  of particle  $m$ , and the vector that connects the centroid of the particle  $m$  to  $\alpha$ .  $k$  is the number of boundary contact points.  $\hat{f}_j^\beta$  and  $x_i^\beta$  are the force acts on the boundary contact point  $\beta$ , and the position vector of this point, respectively.  $x_i^{c_m}$  is the position vector of the centroid of the particle  $m$ .  $p_j$  is the particle surface traction arising from pore pressures and,  $S^m$  is the surface of the particle  $m$ .

For any element in a continuum, the stresses on any plane ( $t_n$ ) can be written as in Equation 5. Figure 5 shows the Cauchy stress components diagrammatically.

$$t_{(n)i} = \tau_{ij} n_j \quad (5)$$

The total stress in the RVE can be defined as the average of stresses acting on the RVE. Li (2003a) used divergence theorem on Cauchy's stress (Equation 6) to correlate the total stresses on the volume of the RVE to the average of the surface tractions ( $T_i$ ) acting on the surface ( $S$ ):

$$\sigma_{ij} \triangleq \frac{-1}{V} \int_V \tau_{ij} dV = \frac{-1}{V} \int_S T_j x_i dV \quad (6)$$

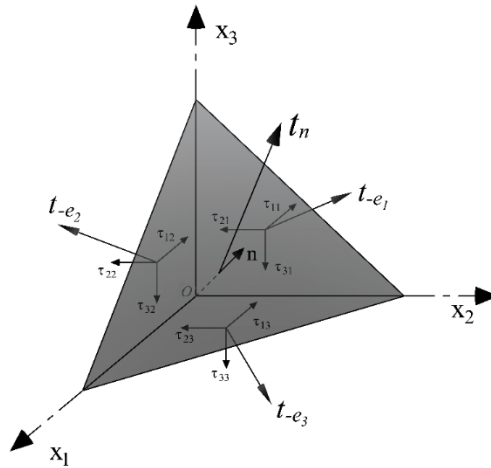


**Figure 5. Components of stress for Cauchy's formula.**

Surface tractions, on the RVE, were taken as composed of three components: pore pressures, boundary contact forces ( $\hat{f}_j^\beta$ ), and surface tension with intensity  $(u_a - u_w) \lambda_i$  that is acting on a perimeter line ( $\Gamma$ ) formed by the liquid-air meniscus (see figure 4c).  $\lambda_i$  defines the properties (i.e. the intensity and direction) of the surface tension. Li (2003a) applied the three components of the surface traction to Equation 6 and formulated the total stress as following:

$$\sigma_{ij} = \frac{-1}{V} \sum_{\beta=1}^k \hat{f}_j^\beta x_i^\beta + u_a \delta_{ij} - (u_a - u_w) \left( S_r \delta_{ij} + \frac{1}{V} \int_{\Gamma} \lambda_j x_i d\Gamma \right) \quad (7)$$

Where  $\delta_{ij}$  is the Kronecker delta, and  $S_r$  is the degree of saturation. Combining Equations 4 and 7, Li (2003a) expressed a quasi-effective stress quantity as:

$$\frac{-1}{V} \sum_{m=1}^{N^p} \sum_{\alpha=1}^{N^m} f_j^{m\alpha} r_i^{m\alpha} = (\sigma_{ij} - u_a \delta_{ij}) + (u_a - u_w) \left( S_r \delta_{ij} + \frac{1}{V} \int_{\Gamma} \lambda_j x_i d\Gamma \right) - \frac{1}{V} \sum_{m=1}^{N^p} x_i^{cm} \int_{S^m} p_j dA \quad (8)$$

The pore pressure ( $p_j$ ) acting on the surface ( $S^m$ ) of particle  $m$  is composed of three components as shown in Figure 6. The first two components are air pressure and water pressure. Figure 6a shows that the difference between air and water pressure on the surface of the particle produces a pressure  $(u_a - u_w)$  around the perimeter of the wet particle surface. Figure 6b shows the air and water pressures acting on the liquid-air meniscus and the resultant force that act along a line that separates the three phases of the unsaturated soil. The interface between air and water phases is called contractile skin (Fredlund and Morgenstern 1977) and this additional force is known as surface tension. Figure 7 shows an analogy between the rope of a hiker, climbing the hillside, and the surface tension produced by  $(u_a - u_w)$ . It can be inferred from the figure that any force that is induced in contractile skin (due to the pressure deficiency), eventually gets transferred to the boundary of the wetted area on the particle surface ( $\Gamma^m$ ).

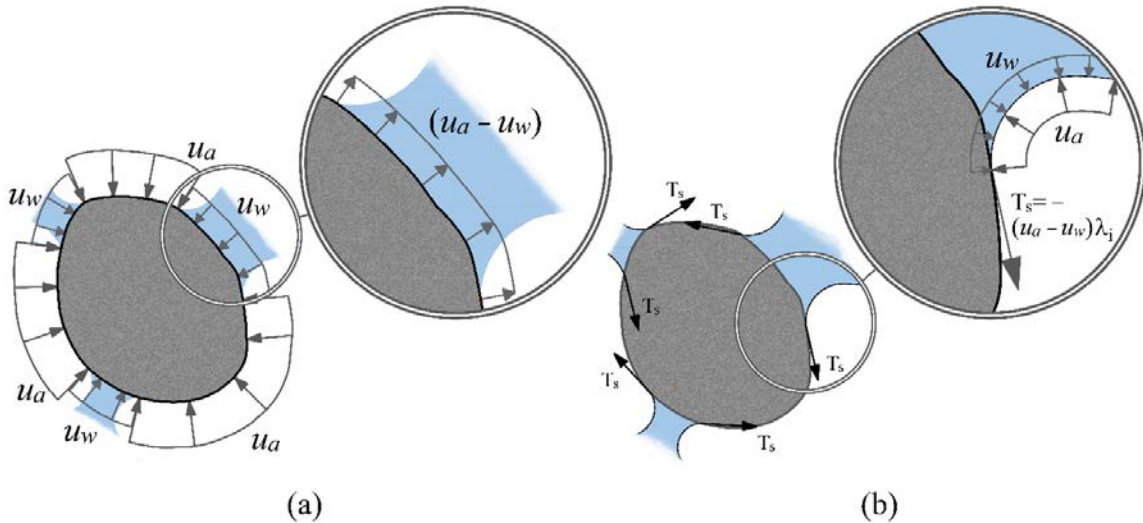


**Figure 6. Components of stress acting on the particle surface.**

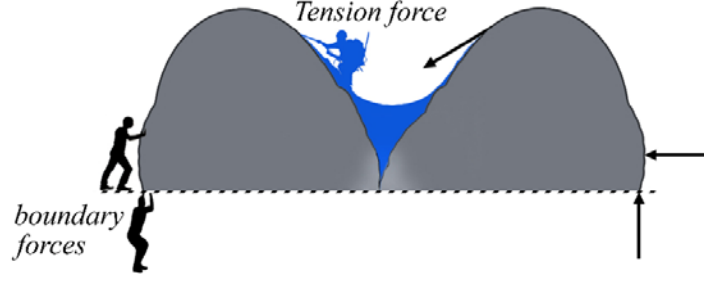


**Figure 7. Analogy between the rope of a hiker and the surface tension.**

Considering the three components of pore pressure acting on particle surface, Li (2003a) evaluated  $p_j$  over the surface particle  $m$  as:

$$\int_{S^m} p_j dA = -u_a \int_{S^m} n_j dA + (u_a - u_w) \left( \int_{S_w^m} n_j dA + \int_{\Gamma^m} \lambda_j d\Gamma \right) \quad (9)$$

Where  $S_w^m$  is the wet surface of the particles. Li (2003a) assumed that the integral of a constant hydrostatic pressure (e.g. air pressure) over the entire surface of a particle is equal to zero. Therefore, equation 10 reduces to:

$$\begin{aligned} \int_{S^m} p_j dA &= -\int_{S_w^m} u_w n_j dA - \int_{S_d^m} u_a n_j dA + (u_a - u_w) \int_{\Gamma^m} \lambda_j d\Gamma \\ &= -u_a \int_{S^m} n_j dA + (u_a - u_w) \left( \int_{S_w^m} n_j dA + \int_{\Gamma^m} \lambda_j d\Gamma \right) \end{aligned} \quad (10)$$

However, the integral  $\int_{S^m} n_j dA$  cannot be ignored without any justification. The authors of this work argue that this integral can be zero only when the particle under consideration has complete symmetry. A 2D illustration of this is shown in figure 8. For the conceptual 2D circular particle shown in Figure 8 (a), there is a counter balance pressure for any pressure located in the circumference of the circle. On the other hand, the horizontal and vertical equilibrium equations are not satisfied for the conceptual 2D triangular particle shown in figure 8 (b).

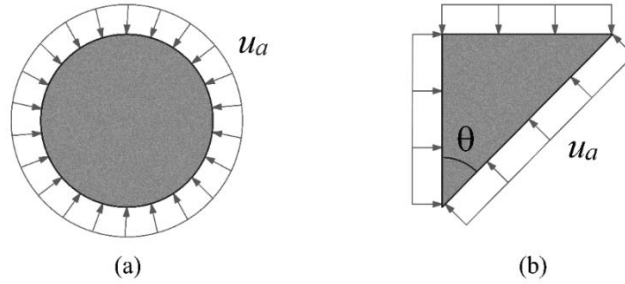


**Figure 8. Integral of hydrostatic pressure over the boundary of (a) circular shape (b) triangular shape.**

Applying Equation 10 into Equation 8 leads to the comprehensive micromechanical formulation for unsaturated soil defined by Li (2003a).

$$\sigma'_{ij} = \frac{1}{V} \sum_{m=1}^{N^p} \sum_{\alpha=1}^{N^m} f_i^{m\alpha} r_j^{m\alpha} = (\sigma_{ij} - u_a \delta_{ij}) + (u_a - u_w) F_{ij} \quad (11)$$

In Equation 11,  $F_{ij}$  was referred to as the fabric tensor and denotes the following:

$$F_{ij} = S_r \delta_{ij} + \underbrace{\frac{1}{V} \sum_{m=1}^{N^p} x_j^{c_m} \int_{S_w^m} n_j dA}_{\text{due to pressure deficiency on particle surface}} + \underbrace{\frac{1}{V} \left( \int_{\Gamma} \lambda_j d\Gamma + \sum_{m=1}^{N^p} x_j^{c_m} \int_{\Gamma^m} \lambda_j d\Gamma \right)}_{\text{due to pressure deficiency in contractile skin}} \quad (12)$$

As can be seen in the expression,  $F_{ij}$  is a function of particle geometry and volumetric quantities such as the degree of saturation. It was shown that fabric tensor of the liquid phase is anisotropic and has an intrinsic association with the evolution of the effective stress tensor Manahiloh et al. (2015). It is also shown that this variation is random and can be depicted by applying techniques of digital image processing.

The intensity and direction of surface tension could not easily be captured with conventional testing and measurements. Manahiloh et al. (2015) assumed that the air-water interface moves with the soil skeleton, and the relative velocity of the contractile skin is negligible or zero. Therefore, the contribution of contractile skin to the virtual work can be ignored (Houlsby 1997). This assumption eliminates the  $\lambda_i$  from the preceding derivation steps. Accordingly, Equation 8 reduces to:

$$\begin{aligned} \sigma_{ij} &= \frac{-1}{V} \sum_{\beta=1}^k \hat{f}_j^{\beta} x_i^{\beta} + u_a \delta_{ij} - S_r \delta_{ij} (u_a - u_w) \\ &= \frac{-1}{V} \sum_{\beta=1}^k \hat{f}_j^{\beta} x_i^{\beta} + \{S_r u_w + (1 - S_r) u_a\} \delta_{ij} \end{aligned} \quad (13)$$

They also assumed that the pore pressure inside the RVE remain the same and defined  $P_j$  as shown in Equation 14.

$$\int_{S^m} p_j dA = \int_{S^m} \{S_r u_w + (1 - S_r) u_a\} n_j dA \quad (14)$$

Applying similar assumptions and equating boundary force contributions derived from virtual work and continuum approaches, the micromechanical effective stress formulation was shown to reduce to:

$$\sigma'_{ij} = \frac{1}{V} \sum_{m=1}^{N^p} \sum_{\alpha=1}^{N^m} f_i^{m\alpha} r_j^{m\alpha} = \sigma_{ij} - [S_r u_w + (1 - S_r) u_a] F_{ij} \quad (15)$$

In this case, the fabric tensor  $F_{ij}$  took the form shown in Equation 16.

$$F_{ij} = \delta_{ij} + \frac{1}{V} \sum_{m=1}^{N^p} x_i^{c_m} \int_{S^m} n_j dA \quad (16)$$

In order to compare Equation 15 with classical macro-mechanical definition of the effective stress, this equation can be rearranged as follows:

$$\sigma'_{ij} = (\sigma_{ij} - u_a F_{ij}) - (u_a - u_w) S_r F_{ij} \quad (17)$$

## THE MEANING OF FABRIC TENSOR

Two micro-mechanical formulation of effective stress, described in previous section, are used to interpret the strength of the granular partially saturated materials. Comparing the bishop type effective stress with Li's equation (Li 2003a) one can surmise that the material parameter defined by bishop depends on the fabric of the water and solid particles:

$$\sigma'_{ij} = (\sigma_{ij} - u_a \delta_{ij}) + (u_a - u_w) F_{ij} = (\sigma_{ij} - u_a \delta_{ij}) + (u_a - u_w) \chi \quad (18)$$

Which immediately suggests that  $\chi$  is direction dependent and equals to the fabric tensor:

$$\chi_{ij} = F_{ij} \quad (19)$$

Substituting this equation to the Mohr-coulomb failure envelope equation yields:

$$\tau_f = c' + \left( (\sigma_{ij} - u_a \delta_{ij}) + (u_a - u_w) F_{ij} \right)_f \tan \phi' = c' + (\sigma_{ij} - u_a \delta_{ij})_f \tan \phi' + (u_a - u_w)_f F_{ij} \tan \phi' \quad (20)$$

Comparing this equation with the extended Mohr-Coulomb criterion, one can reach at a correlation between fabric tensor and the increase in shear strength captured by  $\phi^b$  as:

$$\tan \phi^b = F_{ij} \tan \phi' \quad (21)$$

In order to follow the same procedure for the equation obtained by Manahiloh et al. (2015), Equation 17 can be rearranged as follows:

$$\begin{aligned} \sigma'_{ij} &= (\sigma_{ij} - u_a F_{ij} - u_a \delta_{ij} + u_a \delta_{ij}) - (u_a - u_w) S_r F_{ij} \\ &= (\sigma_{ij} - u_a \delta_{ij}) + u_a (\delta_{ij} - F_{ij}) - (u_a - u_w) S_r F_{ij} \end{aligned} \quad (22)$$

Comparing Equation 22 with bishop's effective stress leads to:

$$\chi_{ij} = u_a (\delta_{ij} - F_{ij}) - (u_a - u_w) S_r F_{ij} \quad (23)$$

Substitution of Equation 23 into the Mohr-coulomb failure criterion, and combining the resulting equation with extended Mohr-coulomb failure envelope equation, one can write:

$$\tan \phi^b = \left( \frac{u_a (\delta_{ij} - F_{ij})}{(u_a - u_w)} - S_r F_{ij} \right)_f \tan \phi' \quad (24)$$

Both Equations 19 and 23 show that the material variable  $\chi$  is direction dependent and needs to be found for the weakest plane.

In Equations 21 and 24, it can be seen that the left hand side of the equations has scalar value while the right hand side shows tensorial characteristics. This imbalance followed from direct comparison of the Extended Mohr-Coulomb equation with Equation 20. However, mathematically, the two sides need to be "equivalent" index-wise. From geotechnical point of view, it can be concluded that  $\phi^b$  is dependent on the evolution of fabric, which is captured by  $F_{ij}$ . Thus Equations 21 and 24 should be modified by accounting this dependence as follows:

$$\left[ \tan \phi^b \right]_{ij} = f(F_{ij}) \tan \phi' \quad (25)$$

If one considers limit equilibrium on the verge of failure, one can expect that the fabric tensor is direction dependent and has principal values (Equation 26) that can be obtained by solving its eigenvalue problem.

$$\begin{bmatrix} F_1 & 0 & 0 \\ 0 & F_2 & 0 \\ 0 & 0 & F_3 \end{bmatrix} \quad (26)$$

Which, according to Equations 19 and 21, leads to the values of  $\chi$  and  $\tan \phi^b$  as given by Equations 27 and 28. Similarly, according to Equations 23 and 24,  $\chi$  and  $\tan \phi^b$  attain the values given by Equations 29 and 30, respectively.

$$\chi = F_3 \quad (27) \quad \tan \phi^b = F_3 \tan \phi' \quad (28)$$

$$\chi = u_a(1 - F_3) - (u_a - u_w) S_r F_3 \quad (29) \quad \tan \phi^b = \left( \frac{u_a(1 - F_3)}{(u_a - u_w)} - S_r F_3 \right)_f \tan \phi' \quad (30)$$

Further investigation of the fabric tensor, requires the development image processing algorithms, and experimental testing systems and their integration with high-resolution CT-scanners to capture the evolution of the fabric during hydro-mechanical loading. The authors hypothesize that the successful implementation of the micromechanically driven equation for effective stress appears pivoted on finding efficient ways of capturing the evolution of the fabric tensor while specimens are loaded to failure. High-resolution X-ray CT image acquisition systems can accommodate large samples and the associated loading set up. Shearing devices such as the traditional triaxial testing device have metallic parts that stand in the way of X-rays and prohibit the acquisition of good resolution images. Such systems could be designed by replacing the metal pieces with high-strength, low-density materials and could be used to overcome the issue of X-ray attenuation on the metal parts. The microstructural information obtained from such loading-imaging integration could help in the micromechanical quantification of the soil behavior.

## CONCLUSIONS

Micromechanical examination of effective stress in unsaturated soils was revisited in this work. The extended Mohr-Coulomb and the effective stress approaches were compared and parameters were interrelated. To this end, two micromechanically driven effective stress expressions were investigated comparatively. Mathematically, it was shown that the conventional material parameters that capture the strength behavior of unsaturated soils are functions of the geometry of the particles and water as described by the fabric tensor. The nonlinearity in the angle of friction associated with matric suction ( $\phi^b$ ) is attributed to the evolution of fabric tensor as the loading conditions and saturation direction (wetting/drying) changes. It was shown that material variables

that characterize the shear strength of an unsaturated soil (e.g.  $\phi^b$  and  $\chi$ ) are direction dependent and could be obtained by evaluating the eigenvalues and eigenvectors of the fabric tensor.

## REFERENCES

- Bishop, A. W. (1959). "The principle of effective stress." *Teknisk Ukeblad*, 106(39), 859-863.
- Bishop, A. W., and Blight, G. E. (1963). "Some aspects of the mechanical behavior of partly saturated soils." *Geotechnique*, 13(3), 177-197.
- Blight, G. E. (1967). "effective stress evaluation for for unsaturated soils." *ASCE journal of the soil mechanics and foundations division*, 93((SM2)), 125-148.
- Fredlund, D. G., and Morgenstern, N. R. (1977). "Stress State Variables for unsaturated soils." *ASCE Journal of Geotechnical Engineering*, 103, 444-466.
- Fredlund, D. G., Morgenstern, N. R., and Widger, R. A. (1978). "Shear strength of unsaturated soils." *canadian Geotechnical Journal*, 15(3), 313-321.
- Houlsby, G. T. (1997). "The work input to an unsaturated granular material." *Géotechnique*, 47(1), 193-196.
- Jennings, J. E. B., and Burland, J. B. (1962). "Limitations to the use of effective stress in partly saturated soils." *Geotechnique*, 12(2), 125-144.
- Li, X. S. (2003a). "Effective stress in unsaturated soil: A microstructural analysis." *Geotechnique*, 53(2), 273-277.
- Manahiloh, K. N., Muhunthan, B., and Likos, W. J. (2015). "Microstructure based effective stress formulation for partially saturated granular soils." *ASCE International Journal of Geomechanics: Special Issues on Experimental and Computational Geomechanics for Unsaturated soils*, 1:13.
- Terzaghi, K. (1925). "Erdbaumechanik auf Bodenphysikalischer Grundlage. Franz Deuticke, Leipzig-Vienna."
- Terzaghi, K. "The shear strength of saturated soils." *Proc., First international conference on soil mechanics and foundation engineering*, 54-56.
- Vanapalli, S. K., Fredlund, D. G., Pufahl, D. E., and Clifton, A. W. (1996). "Model for the prediction of shear strength with respect to soil suction." *Canadian Geotechnical Journal*, 33, 379-392.